Infectious Disease Modelling 8 (2023) 84–100

Contents lists available at ScienceDirect

Infectious Disease Modelling

journal homepage: www.keaipublishing.com/idm

A new mixed agent-based network and compartmental simulation framework for joint modeling of related infectious diseases- application to sexually transmitted infections

Chaitra Gopalappa*, Hari Balasubramanian [1], Peter J. Haas [1]

University of Massachusetts Amherst, 160 Governors Drive, Amherst, MA, 01003, USA

ARTICLE INFO

Article history:
Received 23 October 2022
Received in revised form 14 December 2022
Accepted 15 December 2022
Available online 23 December 2022
Handling Editor: Dr HE DAIHAI

Keywords:
Joint-modeling diseases
Multi-disease modeling
Simulation modeling
HIV and STIs
Diseases and social determinants
SDOH

ABSTRACT

Background: A model that jointly simulates infectious diseases with common modes of transmission can serve as a decision-analytic tool to identify optimal intervention combinations for overall disease prevention. In the United States, sexually transmitted infections (STIs) are a huge economic burden, with a large fraction of the burden attributed to HIV. Data also show interactions between HIV and other sexually transmitted infections (STIs), such as higher risk of acquisition and progression of co-infections among persons with HIV compared to persons without. However, given the wide range in prevalence and incidence burdens of STIs, current compartmental or agent-based network simulation methods alone are insufficient or computationally burdensome for joint disease modeling. Further, causal factors for higher risk of coinfection could be both behavioral (i.e., compounding effects of individual behaviors, network structures, and care behaviors) and biological (i.e., presence of one disease can biologically increase the risk of another). However, the data on the fraction attributed to each are limited.

Methods: We present a new mixed agent-based compartmental (MAC) framework for jointly modeling STIs. It uses a combination of a new agent-based evolving network modeling (ABENM) technique for lower-prevalence diseases and compartmental modeling for higher-prevalence diseases. As a demonstration, we applied MAC to simulate lower-prevalence HIV in the United States and a higher-prevalence hypothetical Disease 2, using a range of transmission and progression rates to generate burdens replicative of the wide range of STIs. We simulated sexual transmissions among heterosexual males, heterosexual females, and men who have sex with men (men only and men and women). Setting the biological risk of co-infection to zero, we conducted numerical analyses to evaluate the influence of behavioral factors alone on disease dynamics.

Results: The contribution of behavioral factors to risk of coinfection was sensitive to disease burden, care access, and population heterogeneity and mixing. The contribution of behavioral factors was generally lower than observed risk of coinfections for the range of hypothetical prevalence studied here, suggesting potential role of biological factors, that should be investigated further specific to an STI.

Conclusions: The purpose of this study is to present a new simulation technique for jointly modeling infectious diseases that have common modes of transmission but varying epidemiological features. The numerical analysis serves as proof-of-concept for the application to STIs. Interactions between diseases are influenced by behavioral factors, are

* Corresponding author.
E-mail address: chaitrag@umass.edu (C. Gopalappa).
Peer review under responsibility of KeAi Communications Co., Ltd.
[1] HB and PJH equally contributed to the work and are listed in alphabetical order.

https://doi.org/10.1016/j.idm.2022.12.003

sensitive to care access and population features, and are likely exacerbated by biological factors. Social and economic conditions are among key drivers of behaviors that increase STI transmission, and thus, structural interventions are a key part of behavioral interventions. Joint modeling of diseases helps comprehensively simulate behavioral and biological factors of disease interactions to evaluate the true impact of common structural interventions on overall disease prevention. The new simulation framework is especially suited to simulate behavior as a function of social determinants, and further, to identify optimal combinations of common structural and disease-specific interventions.

1. Introduction

A model that jointly simulates infectious diseases that have common modes of transmission will be a useful decision-analytic tool to identify optimal intervention combinations for overall disease prevention. In the United States, sexually transmitted infections (STIs) continue to impose high disease and economic burdens. The lifetime medical costs for treatment of STIs and sequelae, for incident infections in 2018, were estimated at $15.9 billion, with a large fraction attributed to human immunodeficiency virus (HIV) infection ($13.7 billion) (Chesson et al., 2021). Further, there are considerable interactions between HIV and other STIs, including human papillomavirus (HPV), hepatitis C (HCV), hepatitis B (HBV), gonorrhea (NG), chlamydia (CT), and syphilis, in terms of HIV acquisition, transmission, or progression as seen in the following examples. The odds of HPV infection, infection with high-risk oncogenic HPV types that lead to cervical cancer, HBV infection, and liver-related mortalities from HCV or HBV are higher in women living with HIV compared to women without an HIV infection (Ferenczy et al., 2003; Liu et al., 2016, 2018; Tartaglia et al., 2017). Among persons with HIV (PWH), the risk of cervical cancer (Ferenczy et al., 2003) and mortality from liver cancer (Thio et al., 2002) were directly correlated with HIV stage. Persons with syphilis, CT, and NG have higher risk of HIV transmission and acquisition (Fleming & Wasserheit, 1999; Heiligenberg et al., 2012). Studies also show higher risk of CT and NG among HIV infected persons who also had a recent HCV infection or syphilis infection (Lin et al., 2021). Further, though there is sufficient evidence associating risk and severity of coinfections to biological factors (i.e., presence of one disease can biologically increase the risk of another), these estimates are confounded by behavioral factors (combined effects of individual sexual behavior, partnership network structure, and care behaviors). Observational studies alone are insufficient to quantify risk attributed to each factor (Jones et al., 2019; Orroth et al., 2006).

A model that can jointly simulate STIs can quantify risk of disease attributable to behavioral and biological factors, determine intervention needs, and jointly evaluate interventions for overall disease prevention. Interventions to address biological factors include disease management interventions, such as pharmaceutical and care support programs. On the other hand, structural interventions, such as health care coverage, subsidized housing, childcare and food programs, access to mental healthcare, and early childhood academic enrichment programs (Adimora & Auerbach, 2010; Blankenship et al., 2000, 2006; Frieden, 2010; Sipe et al., 2017) are key part of behavioral interventions. This is due to the fact that social and economic conditions are among key drivers of behaviors associated with STI transmission, e.g., higher number of partners, higher rates of condomless sex, higher rates of substance abuse, and lower care access among people experiencing homelessness compared to those stably housed (Craddock et al., 2020; Edidin et al., 2012; Henwood et al., 2020; Maria et al., 2020). Consequently, social determinants are key correlates of disease burden. Among persons living with diagnosed HIV infection, 44% had a disability (including physical, mental, and emotional disabilities), 41% were unemployed, 43% had household incomes at or below the federal poverty threshold, and 10% were experiencing homelessness (cdc-hiv-surveillance-special-report-number-25.pdf, 2021; Huang et al., 2015). A joint disease model, that simulates disease interactions through the behavioral factors that are common modes of transmission, will be ideal to simulate behaviors as functions of social determinants, and eventually, serve as a decision-analytic tool for identifying the most cost-effective combinations of disease-specific and common structural interventions for overall STI prevention.

Multi-disease models in the literature are limited, and most focus on chronic diseases prediction (Paul et al., 2014; Walker et al., 2013, p. 17) or management (Damery et al., 2015; Jeon et al., 2012; McPhail, 2016). Some focus on infectious diseases, but use a single simulation technique (Bershteyn et al., 2018; Jones et al., 2019; Lauer et al., 2003; Orroth et al., 2006) which is not computationally sufficient for modeling diseases of widely varying incidence and prevalence. Other models only do combined health infrastructure costing of diseases without modeling disease interactions (World Health Organization, 2013). Among commonly used simulation techniques, compartmental modeling is sufficient for fast-spreading or high-prevalence infections, whereas agent-based network modeling (ABNM) is preferred for slower-spreading, lower-prevalence infections, where granular representations of network structures and individual-level characteristics are key for accurate estimations (Smieszek et al., 2009). Even ABNM, however, becomes computational challenging to use for diseases with very low prevalence, such as HIV in the United States. Thus, in our previous work, we developed an agent-based evolving network modeling (ABENM) technique, which uses a hybrid ABNM and compartmental structure for single disease modeling of lower-prevalence diseases (Eden et al., 2021). This simulation technique was applied to develop PATH 4.0 (Progression and

Transmission of HIV), a comprehensive simulation model of HIV in the United States that was validated against metrics from the National HIV Surveillance System (NHSS) for the period 2006 to 2017(33). While HIV, HBV, HCV, and syphilis are slower-spreading, lower-prevalence diseases, HPV, NG, and CT are faster-spreading higher-prevalence diseases (Kreisel et al., 2018). Therefore, ABNM or ABENM alone will not be sufficient for co-modeling of these diseases, due to computational challenges (discussed in Methods) arising from co-modeling widely varying disease burdens in a national context. We developed a mixed agent-based compartmental (MAC) framework that uses ABENM for lower-prevalence diseases and compartmental model for higher-prevalence diseases.

This paper presents the MAC mathematical framework for multi-disease modeling. We demonstrate the framework by applying it to the case of two-disease modeling, representing Disease 1 via ABENM and Disease 2 via compartmental modeling. We adopt the PATH 4.0 model to represent HIV as lower-prevalence Disease 1, and we construct a hypothetical higher-prevalence Disease 2, evaluating it with a range of values for epidemiological parameters to generate incidence and prevalence representative of the wide range of STIs. Further, we conduct numerical analyses to quantify the risk of coinfection attributable to behavioral factors alone, assessing its sensitivity to disease burden, care access, and population heterogeneity. This paper serves as proof-of-concept for the MAC framework, to demonstrate its feasibility and to highlight, through the numerical analyses, the potential significance of joint modeling of diseases.

2. Methods

Fig. 1 gives an overview of the MAC framework, which employs the ABENM-based PATH 4.0 model of HIV(33). The main concept of ABENM as used in PATH 4.0 is to simulate persons infected with HIV and their immediate contacts as individual agents and all other persons using a compartmental model. Immediate contacts are defined as all sexual partners a person will have over their lifetime; at the current time-step they could either be infected or susceptible. In-turn, as these susceptible contacts in the network become infected with HIV, their immediate contacts are added as agents to the network (transitioning from the compartmental portion of the model to the network portion of the model), thus *evolving the contact network*. An Evolving Contact Network Algorithm (ECNA) maintains the network dynamics.

The MAC simulation framework expands on the above concepts of ABENM, where all persons in a population are either in a network or in a compartmental model. To accommodate the multiple diseases, it simulates only persons infected with at least one lower-prevalence disease and their immediate contacts as agents in a network, and it simulates all other persons, including those infected with only higher-prevalence diseases, via a compartmental model (see Fig. 1). As the exposed immediate contacts of agents in the network become infected with a lower-prevalence disease, their contact network is generated by moving persons from the compartmental model to the network using the ECNA. As HIV or HCV are slower-spreading lower-prevalence diseases in the United States, with an annual incidence at 13 and 1, respectively, per 100,000 persons in 2018 (Fig. 2a) (Kreisel et al., 2018), they are suitable candidates for ABENM. As HPV, CT, or GN are faster-spreading higher-prevalence diseases in the United States, with annual incidence at 1820, 640, and 212, respectively, per 100,000 persons in 2018 (Fig. 2a) (Kreisel et al., 2018), they are suitable candidates for compartmental modeling. The MAC framework would be computationally advantageous over ABNM for jointly modeling these diseases that have varying epidemiological features. For example, in ABNM, simulating 100,000 nodes in the network representative of the sexually active population in the United States will generate sufficient samples for the higher-prevalence disease, but for lower-prevalence HIV it would

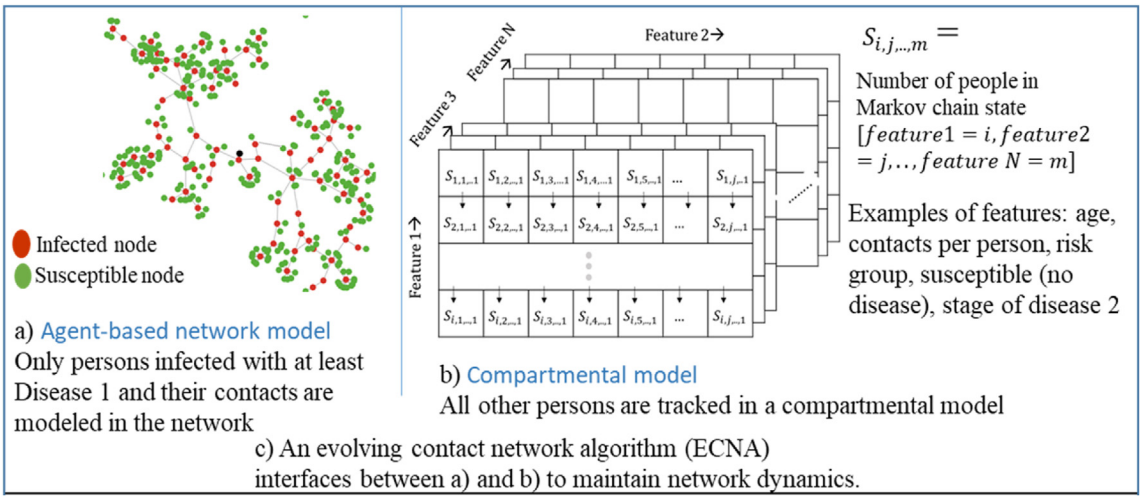

Fig. 1. Computational structure of mixed agent-based compartmental(MAC) simulation framework for multi-disease modeling, taking two diseases for illustration, a low prevalence Disease 1 and a higher prevalence Disease 2.

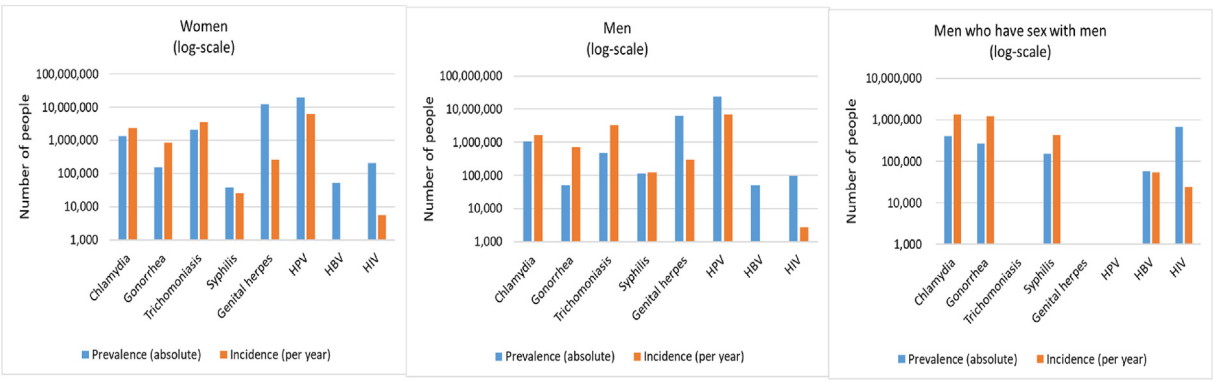

Fig. 2a. Prevalence (absolute) and incidence (per year) of STIs in the US [Source (Chan et al., 2016; Kreisel et al., 2018; Ong et al., 2019; Purcell et al., 2012; Tsuboi et al., 2021; Werner et al., 2018):]. *Note: Except for HIV, all other STI incidence in MSM (men who have sex with men) were among MSM at high-risk of STI from pooled global estimates; Not all STI are presented for MSM due to data unavailability.*

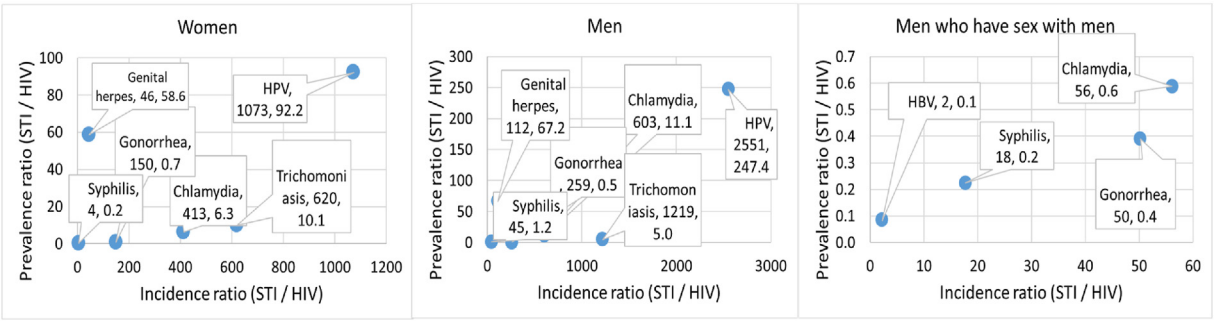

Fig. 2b. STI to HIV incidence ratios (x-axis) and prevalence ratios (y-axis) for common STIs in the U.S. in 2018 [Source (Chan et al., 2016; Kreisel et al., 2018; Ong et al., 2019; Tsuboi et al., 2021; Werner et al., 2018):]. *Note: Except for HIV, all other STI incidence in MSM (men who have sex with men) were among MSM at high-risk of STI from pooled global estimates; Not all STI are presented for MSM due to data unavailability.*

generate 490 persons with HIV with 13 new cases each year, which is not a sufficient sample size for our analyses. In contrast, in ABENM, as the network will consist of only persons with the lower-prevalence disease and their partners, the population size in the network can be controlled to meet computational needs without compromising the sample size of either disease. As an example, we can generate the network with a sufficient but computationally efficient sample of HIV infected persons, say 12,000 (as was the case in our numerical analyses), as a scaled representation of the 0.4% HIV prevalence in 2017 in the United States (Centers for Disease Control and Prevention, 2015), which is equivalent to simulating a population size of ~3 million (compartmental plus network).

2.1. Overview of MAC

We present an overview of the MAC simulation framework, using, without loss of generality, a two-disease example, lower-prevalence Disease 1 and higher-prevalence Disease 2. An overview of the MAC simulation framework is presented in Fig. 1 using, for illustration, two diseases, Disease 1 is tracked in a network model and Disease 2 is tracked through a compartmental model. We describe below an overview of the model and present its mathematical formulations in the Appendix.

2.1.1. Computational structure of MAC

We present below a brief description of the MAC computational structure and present its mathematical representation in Appendix S1.1 and S1.2. We track Disease-1-infected persons and immediate contacts using a dynamic graph $G_t(\mathcal{N}, \mathcal{E})$, with the number of nodes $Q_t = |\mathcal{N}(G_t)|$ and the number of edges $|\mathcal{E}(G_t)|$ in the graph dynamically changing over time t as persons become newly infected with Disease 1 and their immediate contacts are added to the network. Each person in the network has attributes such as age, HIV transmission category (heterosexual males, heterosexual females, men who have sex with men), degree (number of lifetime partnerships), geographic jurisdiction, and health status ({stage of Disease 1, stage of Disease 2}, including {0, 0} to indicate uninfected with either disease).

We track all other persons using an array S_t of size $A \times R \times D \times G \times H$ (our numerical analyses uses $7 \times 3 \times 9 \times 1 \times 2$), where, A is the number of age-groups, R is the number of risk-groups, D is the number of degree-bins (degree is the number of contacts per person, degrees are grouped into bins analogous to age grouped into age-groups), G is the number of geographic jurisdictions (in our numerical analyses we assumed $G = 1$, corresponding to a national jurisdiction), and H is the number of health states (note: here the size would be equal to the number of Disease 2 health states because, by design, persons infected with Disease 1 will be in the network and thus all persons in the compartmental model will have a value of 0 for Disease 1). Each element of the array $(S_t[\overline{a}, r, \overline{d}, g, h])$ is the number of people in that specific category. We use a dash for age-group and degree-bin notations to indicate that they are grouped intervals in the compartmental model, unlike in the network where each node has a discrete value. A summary list of notations is presented in Appendix Table S1.

Thus, $Q_t + \sum_{i \in [\overline{a}, r, \overline{d}, g, h]} S_{t,i}$, denotes the total number of people in the population at time t. Because all Disease 1 infected persons and exposed partners are in the network, Disease 1 transmissions and state progression are modeled at the individual level (see network transmission and network disease progression modules below and in Appendix Section S2.2). Disease 2 transmissions and progression are modeled using differential equations (as typically done in compartmental modeling) but with the consideration that people in both the network $G_t(\mathcal{N}, \mathcal{E})$ and compartmental array S_t can be infected with Disease 2 (see compartmental module below and in Appendix Section S2.1).

The mathematical challenge to address for the above MAC framework to work is to maintain the dynamics between the network $G_t(\mathcal{N}, \mathcal{E})$ and compartmental array S_t, including transitioning people from S_t to $G_t(\mathcal{N}, \mathcal{E})$ when a node becomes newly infected. Specifically, the simulation algorithm must determine 'who' are to be added as the immediate contacts of the node newly infected with Disease 1. Here we determine 'who' according to their degree, transmission group, age, and geographical location, as these characteristics of infected persons and their contacts are known to be correlated (Board et al., 1999; Finlayson et al., 2011; Friedman et al., 2014; Glick et al., 2012; Liljeros et al., 2001; Voetsch et al., 2012). Upon determining and adding all lifetime partners of nodes newly infected with Disease 1, we need to determine when the partnerships would initiate and dissolve, including the age of both partners at that time, such that the overall dynamics of age-mixing and transmission-group-mixing of the resulting network match that of the population being simulated. As network generation techniques in commonly used agent-based models are designed to generate the network between the full population (susceptible and infected persons), they cannot be adopted here. We developed an evolving contact network algorithm (ECNA(32,33)) for modeling the transitions from S_t to $G_t(\mathcal{N}, \mathcal{E})$ (see ECNA module below and in Appendix Section S2.3). For diseases that are chronic (such as HIV) once persons enter the network $G_t(\mathcal{N}, \mathcal{E})$ they do not transition back to S_t. For diseases with recovery, recovered persons with no infected contacts can be added back to the compartments corresponding to their categorical group (see (Eden et al., 2021) for stability of network dynamics under different epidemic profiles).

2.1.2. The four main modules of MAC

The overall epidemiological, demographical, and network dynamics are maintained through simulation of four main modules that are run at every time-step (monthly) of the simulation: compartmental module, network transmission module, ECNA network generation module, and network disease progression module.

The formulation of the compartmental module for a hypothetical Disease 2 is presented in Appendix S2.1, we provide a brief overview here. The compartmental module updates the demographic features (births, aging, and deaths) and transmission and progression features of higher-prevalence diseases (Disease 2 here) among persons tracked through the array S_t and in the network $G_t(\mathcal{N}, \mathcal{E})$, as follows. As in typical compartmental modeling, it uses difference equations to transition persons between the compartments. It also determines transitions of the network nodes from one state to another. It does so by converting transition rates to transition probabilities by assuming that sojourn times follow an exponential distribution, as typically done in Markov chains. Then, for every state transition, the module uses the corresponding probability as a parameter of a binomial distribution to determine the number of persons to transition, and it randomly samples that many people from the network who are in the reference state and moves them to the next state. With this approach, the same level of granularity is applied to persons in the network and compartmental models, e.g., in the above representation, the granularity in the compartmental model is $[\overline{a}, r, \overline{d}, g, h]$ and thus the rates would be applied specific to age-group, transmission-group, degree-bin, geographic location, and health state. A key feature of this setup is approximating network features into the compartmental modeling structure. This is done by splitting the compartments into degree-bins ($\overline{d}$, a dimension in array S_t) and using a degree-mixing matrix to simulate partnership mixing between people in different degree-bins. As noted earlier, degree between partners are correlated (Liljeros et al., 2001), and thus this feature helps better capture the network dynamics even in the compartmental model. Whereas the distributions for partnership mixing by age, transmission group, and degree are applied at the individual-level in the network, they are applied at the aggregated-level in the compartmental model.

The network transmission module determines if nodes exposed to a lower-prevalence disease (Disease 1 here) become infected using an individual-level Bernoulli transmission equation. Transmissions are determined at the individual-level using the network structure and individual-level sexual behaviors and transmission risk factors. Thus, the granularity of transmissions can be controlled by modifying the individual-level attributes that are tracked among agents. As an example, Appendix S2.2 presents a Bernoulli transmission equation using the level of granularity applied in the PATH 4.0 model. Note that, by definition, as persons in the compartmental model are not partners of any person infected with the lower-prevalence diseases (Disease 1 here), their chance of infection is zero. Further note that persons can move from the compartmental model

to the network (see Fig. 1) if their partners become infected with Disease 1, modeled using the ECNA module (below), which would then expose them to Disease 1.

The ECNA module controls the overall network dynamics of partnerships between nodes. Specifically, for every node newly infected with Disease 1 in the network, it determines the number of new partnerships to generate and the features of each of those new partners, including their degree (number of lifetime partners), their transmission-group, and their current age-group. The module then randomly selects susceptible persons who meet these criteria and moves them from the compartmental model to the network. The ECNA module also determines partnership details, such as the age of both partners and simulation times at partnership initiation and termination. Three main algorithms were used in the development of this module, which were presented elsewhere (Eden et al., 2021; Singh et al., 2021), and are briefly summarized below and discussed in Appendix S2.3. The first algorithm determines the degree of the new partner using a neural network prediction model, a machine learning method, developed based on the assumption that sexual partnerships are scale-free networks with power-law distribution. For scale-free networks, the degree of node-neighbors are correlated, i.e., in the context here, the degree of the new partner is conditional on the degree of the newly infected node. While the literature presents analytical methods for estimation of the conditional distribution, they are developed for static networks, and thus, the degree of any node is conditional on the degree of 'all' its neighbors. In the evolving network here, the degree of the new partner is conditional on only the degree of the newly infected node, i.e., dependent on the network path taken to reach this person, and thus, the degree correlation is also influenced by the stochastic process of disease transmissions. Our previous work showed that, given a specific network, the degree correlations are not influenced by variations in the probability of transmission but influenced by the prevalence of disease, and thus, trained the neural network by generating the data through multiple simulations of hypothetical diseases, characterized by different values of probability of transmission (Eden et al., 2021). Upon determining the degree of the new partner, the second algorithm is applied to determine the age at which each of those partnerships are active, including the age of the other person in each partnership (one of those partnerships is with the newly infected node). Direct data for this would be a longitudinal survey over the duration of life of an individual, where the individual reports the number of partnerships they initiated at every age points of their life, and the age of their partner. Such surveys, however, are unavailable. Typical survey data only collect the number of partners up to the current age of the surveyed individual, and age of partners at a cross-sectional time-point. By assuming the number of partners up to the current age are steady state distributions of a time-invariant Markov chain with a multivariate state space of age-group - degree-bin combinations (time-invariant from assumption of no generational changes in partnership behavior), the transition probabilities were solved using simulation-based optimization to determine the number of new partnerships initiated in each age-group, for each degree-bin. The third algorithm determines the age-groups of both partners at the time of partnership activation by formulating the problem as a variant of an unbalanced assignment problem, a category of optimization problems with a classic example being assigning n jobs (here partners) to m machines (here age-groups), applying age-mixing matrix and number of partners in each age-group as constraints. Further details of the three algorithms and data assumptions are presented in Appendix S2.3 and S3, respectively.

Finally, the network disease progression module updates the individual-level demographic and disease dynamics for every person infected with Disease 1 (and other low-prevalence diseases as the case may be) in the network. The level of granularity for disease progression could be dependent on the analyses and diseases of interest.

Appendix S4 provides further details on model initialization and S5 gives a more detailed description of the steps of the simulation.

2.2. Numerical analyses

Using the MAC simulation framework, we conducted numerical analyses, using *relative prevalence (RP)* metrics, to quantify the risk of coinfection attributable to behavioral factors (individual sexual behaviors, partnerships networks, and care behaviors) alone. Further, we evaluated the sensitivity of relative prevalence to variations in care access, disease burdens (incidence and prevalence), and population heterogeneity by estimating *RP*metrics specific to transmission group and under varying hypothetical assumptions of care and epidemiological assumptions. For these analyses, we adopted the validated HIV model from PATH 4.0 as Disease 1 and constructed a hypothetical Disease 2 using a compartmental model. To keep the focus on behavioral factors, we assume no biological risk of coinfection, i.e., Disease 1 does not biologically increase the risk of Disease 2, and vice-versa. We first give a brief overview of Disease 1 (HIV) and Disease 2 modeling, and then discuss the numerical analysis in detail.

2.2.1. Overview of HIV (disease 1) model

For the development of MAC, we directly adopted the HIV model from PATH 4.0, which has been validated to match well against data from the CDC's National HIV Surveillance System (NHSS) for both population epidemic features and HIV-network features. Details of PATH 4.0 and its validation are presented elsewhere (Singh et al., 2021); we give a brief description below. PATH 4.0 simulates sexual transmission of HIV in the United States in three transmission categories: heterosexual females (HETF), heterosexual males (HETM), and men who have sex with men (MSM). (Note that MSM includes men who have sex with men only and men who have sex with men and women). To validate the model, we first generated an initial population that is representative of PWH in the United States in 2006 using data from several studies. These include demographical, sexual behavioral, clinical, and HIV care and treatment behavioral studies that originated from multiple large national

surveillance and survey systems in the United States, along with other small studies. The surveillance and survey systems include the National HIV Surveillance System (NHSS), the Medical Monitoring Project (MMP), the HIV Outpatient Study (HOPS), the National HIV Behavioral Surveillance (NHBS), the National Survey for Family Growth (NSFG), and the National Survey for Sexual Health and Behavior (NSSHB) (Broz et al., 2009; Buchacz et al., 2012; Centers for Disease Control and Prevention, 2022a; Centers for Disease CPrevention, 2010; Chandra et al., 2011; Reece et al., 2010). The model was validated for the period 2006 to 2017 by calibrating to 2006 data, simulating the epidemic from 2006 to 2017 in monthly-time steps, and comparing simulated estimates for multiple epidemic features and HIV-network features against data from NHSS. Details of this validation study are presented elsewhere (Singh et al., 2021).

2.2.2. Overview of disease 2 model

Individual sexual behaviors and partnership networks do not change specific to disease, and thus, sexual behavioral data for Disease 2 are the same as in HIV, though in aggregated form for the compartmental model structure. Specifically, individual sexual behaviors such as the number of lifetime partners, distribution of these partnerships over the lifetime of the person (as they transition across age-groups), number of sex acts, and condom use, most parameters specific to transmission group (HETF, HETM, and MSM) and age-group, and sexual network structures such as degree mixing matrix, age-group mixing matrix, and transmission-group mixing matrix to model mixing between partnerships, were adopted from PATH 4.0 (Broz et al., 2009; Buchacz et al., 2012; Centers for Disease Control and Prevention, 2022a; Centers for Disease CPrevention, 2010; Chandra et al., 2011; Reece et al., 2010). Note that, behaviors that change specific to disease can be added over general population behaviors, e.g., change in condom-use behavior upon awareness of HIV status was added to HIV-agents. While behaviors were simulated at the individual-level for HIV, they were simulated at the aggregated-level for Disease 2 in the compartmental model, using corresponding principles of each type of simulation method. That is, in the network, each person was assigned characteristics such as age, transmission -group, and degree, matrices defining mixing between these groups were used for generating their network, and behavior modeled as a function of these characteristics to determine the probability that a susceptible person becomes infected. Whereas, in the compartmental model, compartments define age-group, transmission-group, and degree-bin combinations, and behaviors specific to these compartments and matrices defining mixing between these compartments were included into infection rate estimations (see Appendix S2.1 for methodological details). Infection rates were then used for determining the number of people to transition from susceptible to infected. Demographic features, such as the population sizes of transmission groups (HETF, HETM, MSM), population distributions by age-group, birth rate and natural mortality rates (Age and sex composition in, 2017; Arias, 2004; Purcell et al., 2012), which are not disease-specific, are a feature of the population modeled, and thus the overall model (network + compartmental) would match population features. As noted under Disease 1 overview, these data were comprehensively informed through numerous data sources, estimation methods, and validation processes and are presented elsewhere (Eden et al., 2021; Singh et al., 2021).

The only change for Disease 2 would be its epidemiology. While HIV is a Susceptible-Infected epidemiology structure, i.e., persons live with the infection for the remaining duration of life, we assumed Disease 2 to be a Susceptible-Infected-Susceptible epidemiology structure, i.e., persons can recover from Disease 2 and become susceptible for reinfection, which is representative of higher-prevalence STIs. Transition from Susceptible to Infected stage for Disease 2 would use the same sexual behaviors as in HIV, as noted above, except for the per contact transmission rate which is an epidemiologic parameter specific to a disease. The duration of the Infected stage (transition from Infected to Death) for HIV is an outcome of simulating HIV-disease stage progressions using care data specific to the United States (such as rates of diagnosis, linkage to care, and treatment), in addition to natural disease progression rates. For Disease 2, we used an overall rate of recovery that transitions persons from the Infected to the Susceptible stage, but we did not model sequelae. Thus, the inverse of the recovery rate represents the average duration of Infected stage, reflective of the natural disease progression and care access.

Therefore, there are only two parameters specific to Disease 2, transmission rate and recovery rate, which can be varied to generate diseases of differing incidence and prevalence. As described in the next section, we evaluated 16 scenarios using different combinations of these rates, to generate incidence and prevalence replicative of the range corresponding to STIs observed in the United States.

2.2.3. Metrics and scenarios

For the numerical analysis, we calculated the following metrics:

- The *relative prevalence of D2 given D1* ($RP_{D2|D1}$), estimated as the prevalence of Disease 2 among persons with HIV compared to persons without HIV, i.e.,

$RP_{D2|D1} = \frac{\#\ of\ persons\ with\ Disease\ 2\ and\ HIV\ /\ \#\ of\ persons\ with\ HIV}{\#\ of\ persons\ with\ Disease\ 2\ only(no\ HIV)/\ \#\ of\ persons\ with\ no\ HIV}$, and therefore, if $RP_{D2|D1} > 1$, then persons with HIV have a higher burden of Disease 2 than persons without HIV.

- The *relative prevalence of D1 given D2* ($RP_{D1|D2}$), estimated as the prevalence of HIV among persons with Disease 2 compared to persons without Disease 2, i.e.,

$RP_{D1|D2} = \frac{\#\ of\ persons\ with\ Disease\ 2\ and\ HIV / \#\ of\ persons\ with\ Disease\ 2}{\#\ of\ persons\ with\ HIV\ only\ (no\ Disease\ 2) / \#\ of\ persons\ with\ no\ Disease\ 2}$, and therefore, if $RP_{D1|D2} > 1$, then persons with Disease 2 have a higher burden of HIV than persons without Disease 2.

- The average degree (average number of partners) among all persons with HIV (d_{HIV+}), average degree among all persons with Disease 2 (d_{D2+}), and average degree in the overall population ($d_{Overall}$), which are metrics representing network features.

When estimating $RP_{D2|D1}$ and $RP_{D1|D2}$, we assume no biological risk of coinfection, i.e., Disease 1 does not biologically increase the risk of Disease 2 acquisition, transmission, or progression (and vice-versa). Thus, if $RP_{D2|D1} > 1$ or $RP_{D1|D2} > 1$, it would be attributed to behavioral factors alone, which would be the combined effects of individual-behaviors, partnership network structures, and care behaviors. Note that the assumption of no biological risk is made for purposes of evaluating risk attributed to behavioral factors alone, during application of model in future work, biological risk can be easily modeled by using a multiplier for transmission or disease progression rates.

We report average results for the last year of the simulation (year 2017). Note, over the period 2006 to 2017 (simulation timeline) due to variations in care access (proportion of PWH on treatment with viral suppression increased from ~20% in 2006 to ~56% in 2017(43)) incidence from sexual transmissions decreased from ~44,000 in 2006 to ~33,100 in 2017 (Centers for Disease Control and Prevention, 2022b; Prejean et al., 2011). However, hypothetical D2 is in equilibrium due to the nature of its SIS epidemiology structure.

Prevalence of HIV and care access in the United States has been continuously increasing over the past few decades as noted above (Centers for Disease Control and Prevention, 2015; Centers for Disease Control and Prevention, 2018; Centers for Disease CPrevention, 2011). Further, there is considerable heterogeneity in disease burden, care access, and sexual behavior across transmission risk-groups that mix with each other, thus generating cross-over effects. Therefore, in addition to estimating the risk of co-infections attributable to behavioral factors, we evaluate the sensitivity of relative prevalence to care metrics, disease burden, and population heterogeneity under mixing. The effects of each subcomponent on the relative prevalence metrics are not independent, nor is their effect static over time. Thus, fully evaluating the sensitivity of each will not be feasible. Here, we attempted to gain general insight by utilizing naturally observed variations of these components in the United States. Specifically, we estimated relative prevalence metrics specific to transmission group (sexual behaviors and network structures are inherently different across HETF, HETM, and MSM), under varying epidemiological assumptions for HIV (utilizing the inherent increases in HIV disease burden (Centers for Disease Control and Prevention, 2015; Centers for Disease Control and Prevention, 2018; Centers for Disease CPrevention, 2011) and care access over the past two decades (Bingham et al., 2021; Centers for Disease Control and Prevention, 2013; Centers for Disease Control and Prevention, 2017; Centers for Disease Control and Prevention, 2022c)), under hypothetical assumptions for Disease 2 epidemiology (generating disease burdens replicative of the range observed in STIs in the United States), and under varying assumptions of epidemiology across transmission-groups (utilizing the inherent heterogeneity across risk-groups and mixing of MSM with other MSM and women).

In total, we simulated four scenarios (Scenarios 1 to 4) related to HIV disease burden, and under each, sixteen scenarios related to hypothetical Disease 2 burden, simulating both diseases among three transmission-groups, HETF, HETM, and MSM who have varying individual sexual behaviors and network structures. However, across scenarios, transmission-group specific individual sexual behaviors and network structures, and mixing between transmission-groups remain unchanged, and were comprehensively informed through national surveillance and survey systems in the United States, as noted earlier. We simulated each scenario for a 12 year period. Scenario 1 is a status-quo representation of HIV in the United States for the period 2006 to 2017, and Scenarios 2 to 4 are hypothetical, as follows.

HIV scenarios

- *Scenario 1(status-quo HIV)* was a status-quo representation of HIV in the United States between 2006 and 2017, calibrated to HIV prevalence and HIV care metrics (such as proportions aware, linked to care, and on treatment) specific to transmission group (HETF, HETM, MSM). The model was initiated in 2006, with an HIV prevalence of about 0.1%, 0.05%, and 6% for HETF, HETM, and MSM, respectively, and the proportion of PWH on treatment with viral suppression of about 20%, 18%, and 19%, for HETF, HETM, and MSM, respectively. By 2017, HIV prevalence in the U.S. increased to 0.12%, 0.06%, and 8% for HETF, HETM, and MSM, respectively, and the proportion of PWH on treatment with viral suppression increased to 56%, 50%, and 57%, for HETF, HETM, and MSM, respectively.
- *Scenario 2 (low HIV prevalence low care)* initiates the model with a lower HIV prevalence (taking data from 1990s) of 0.07%, 0.04%, and 3.2% for HETF, HETM, and MSM, respectively, and for the full duration of the simulation (12 years) maintains care metrics to keep the proportion on treatment with viral suppression at a constant value of 20%, 18%, and 19%, for HETF, HETM, and MSM, respectively (corresponding to 2006 care data).
- *Scenario 3 (low HIV prevalence high care)* is similar to Scenario 2 in initiating the model with the low HIV prevalence, but assumes higher care by using care data from 2017, thus resulting in lower HIV incidence compared to Scenario 2. Specifically, the model initiates with a HIV prevalence of 0.07%, 0.04%, and 3.2% for HETF, HETM, and MSM, respectively, and for the full duration of the simulation, maintains care metrics to keep the proportion on treatment with viral suppression at a constant value of 56%, 50%, and 57%, for HETF, HETM, and MSM, respectively.

- *Scenario 4 (equal and low HIV prevalence for all transmission groups)* is similar to Scenario 2 in the use of the 2006 care data, but the model is initiated with equal and low HIV prevalence(1990s HETF prevalence) for all three transmission-groups. Specifically, the model is initiated with a prevalence of 0.07% for HETF, HETM, and MSM, and for the full duration of the simulation, maintains care metrics to keep the proportion on treatment with viral suppression at a constant value of 20%, 18%, and 19%, for HETF, HETM, and MSM, respectively. As the actual prevalence of HIV among MSM has been significantly higher than heterosexuals (HETF and HETM), and as MSM mix with men and women, comparing Scenario 4 with Scenario 2 will provide insight into the sensitivity of the relative prevalence metrics to heterogeneity in populations that mix.

Disease 1 scenarios are summarized in Table 1. In addition to a dry run, that initializes network dynamics and individual-level event history and populate the initial HIV prevalence and care metrics (Appendix S4), we ran each scenario for a period of 12 years and report results for the last year of the simulation.

Disease 2 scenarios. Under each of Scenarios 1 to 4, we simulated 16 scenarios for Disease 2 using combinations of transmission rates (0.04, 0.06, 0.1, 0.2 per contact), and recovery rates (0.042, 0.083, 0.16, and 0.0083 per month, corresponding to an average infection duration of 1, 2, 5 and 10 years, respectively). These values generate a wide range of estimated incidence and prevalence for Disease 2 and were chosen to mimic the range of STIs observed in the United States population (Fig. 2).

3. Results

As expected by design of scenarios, the range of transmission rates and recovery rates used for Disease 2 created epidemics of varying Disease 2 burden, but for a specific combination of transmission rate and recovery rate, Disease 2 burden was similar across all Scenarios 1 to 4 (Fig. 3a). Also as expected by design, Scenarios 1 to 4 created varying Disease 1 (HIV) burdens (Fig. 3b), the values for the last year of the simulation are as follows. Scenario 1 *(status-quo HIV)* had high HIV prevalence for MSM (~8%) compared to heterosexual female (HETF) (~0.12%) and heterosexual male (HETM) (~0.06%), representative of HIV in the United States (Fig. 3b). Compared to Scenario 1, Scenario 2 *(low HIV prevalence, low care)* created a lower HIV prevalence (0.09% for HETF, 0.04% for HETM, and 5% for MSM) but similar incidence because of the low care assumption (Fig. 3b). Scenario 3 *(low HIV prevalence, high care)* created HIV prevalence similar to Scenario 2 but lower incidence because of the higher care assumption. Compared to Scenario 1, Scenario 4 *(low and equal HIV prevalence for all* transmission *groups)* reduced HIV prevalence by an order of magnitude for MSM and, because of mixing between MSM with HETF, reduced HIV prevalence in HETF; HETM had the same prevalence as HETF (0.07% for HETF, 0.06% for HETM, and 0.1% for MSM) (Fig. 3b). As expected from inherent differences in behaviors, and reflecting data inputs to the simulation, the overall average degree ($d_{overall}$) was higher among MSM than HETF and HETM.

Table 1
Overview of Disease 1 (HIV) scenarios.

HIV (Disease 1) scenarios	Descriptive name	HIV prevalence assumptions	HIV care assumptions
Scenario 1	status-quo	Initiated the model with a HIV prevalence of 0.1%, 0.05%, and 6% for HETF, HETM, and MSM, respectively. Values correspond to HIV prevalence in the United States in 2006.	Care continuum distributions scaled-up as per values in the United States over the period 2006–2017. The corresponding values for the proportion of PWH on treatment with viral suppression was about 20%, 18%, and 19%, in 2006, and 56%, 50%, and 57%, in 2017, for HETF, HETM, and MSM, respectively.
Scenario 2	low prevalence, low care	Initiated the model with a HIV prevalence of 0.07%, 0.04%, and 3.2% for HETF, HETM, and MSM, respectively. Values correspond to HIV prevalence in the United States in 1990s.	Care continuum distributions as per values in 2006, and kept constant for all 12 years of simulation. The corresponding values for the proportion of PWH on treatment with viral suppression was about 20%, 18%, and 19%, for HETF, HETM, and MSM, respectively.
Scenario 3	low prevalence, high care	Initiated the model with a HIV prevalence of 0.07%, 0.04%, and 3.2% for HETF, HETM, and MSM, respectively. Values correspond to HIV prevalence in the United States in 1990s.	Care continuum distributions as per values in 2017, and kept constant for all 12 years of simulation. The corresponding values for the proportion of PWH on treatment with viral suppression was about 56%, 50%, and 57%, for HETF, HETM, and MSM, respectively.
Scenario 4	equal and low prevalence for all transmission groups	Initiated the model with a prevalence of 0.07% for HETF, HETM, and MSM. Values correspond to HETF HIV prevalence in the United States in 1990s.	Care continuum distributions as per values in 2006, and kept constant for all 12 years of simulation. The corresponding values for the proportion of PWH on treatment with viral suppression was about 20%, 18%, and 19%, for HETF, HETM, and MSM, respectively.

Note: HIV care assumptions are an input to the simulation. HIV prevalence are an input only for initialization of the model in the first year of simulation. HIV prevalence over time are an outcome of the model. For Scenario 1 (status-quo), the model was validated to match the U.S. epidemic on multiple metrics, including prevalence, for the period 2006 to 2017. Scenarios 2 to 4 are hypothetical.

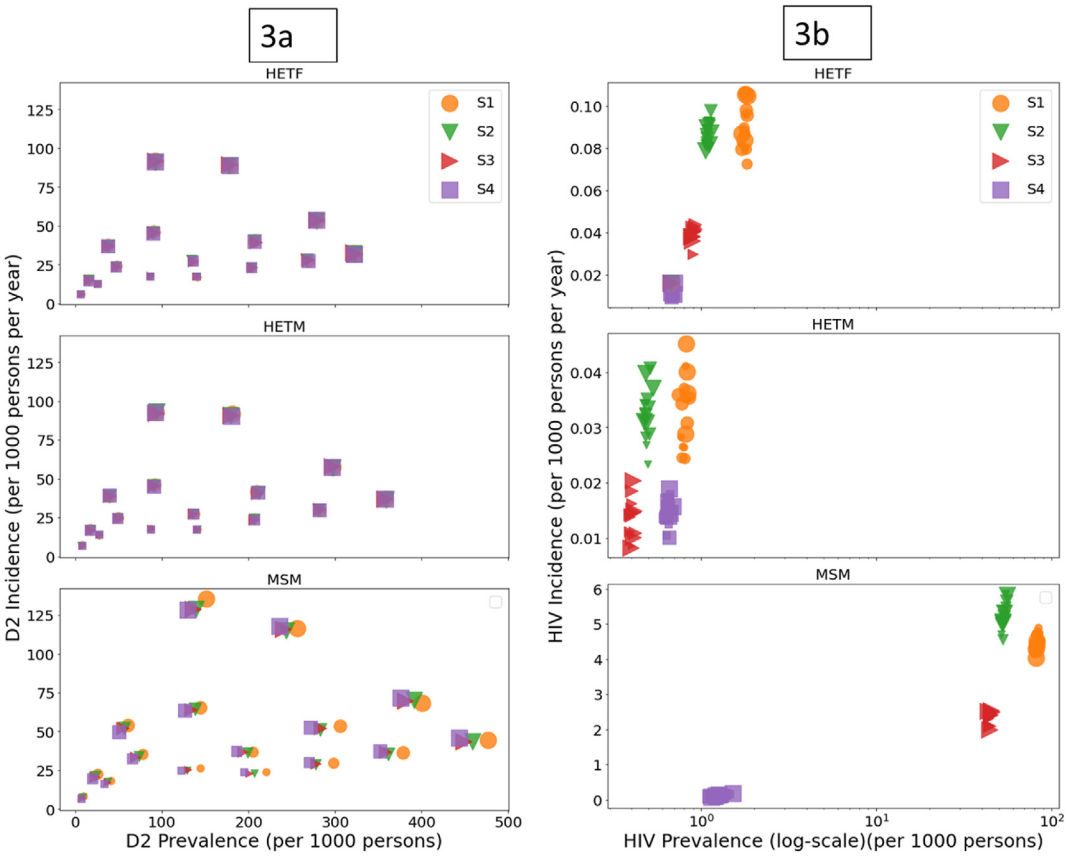

Fig. 3. a) Varying transmission rates and recovery rates creates varying burdens of hypothetical Disease 2 (D2). b) Varying assumptions for HIV across Scenarios 1 to 4 (S1 to S4), creates varying HIV disease burdens (right). *HETF-heterosexual female; HETM-heterosexual male; MSM-men who have sex with men (men only and men and women). Note: For each HIV scenario (S1 to S4), there are 16 data points corresponding to each of the sixteen Disease 2 scenarios (larger the marker size higher the value of D2 transmission rate); For HETF and HETM, data points for S1 to S4 mostly overlap; Results are from last year of 12-year-long simulation (for S1 it corresponds to calendar year 2017).*

$RP_{D2|D1}$ was sensitive to both HIV and Disease 2 burden (incidence and prevalence) and HIV care (Fig. 4a and b), and the patterns could be consistently explained through comparison of resulting average degrees of persons with at least HIV, at least Disease 2, and overall ($d_{HIV+}, d_{D2+}, d_{overall}$, respectively) (Fig. 4c and d). We discuss these below. Keeping HIV prevalence fixed, i.e., observing within each Scenario and transmission-group, as Disease 2 burden increased, $RP_{D2|D1}$ increased. In Scenario 1, $RP_{D2|D1} > 1.2$ for HETF in most cases, $RP_{D2|D1} < 0.8$ for HETM in most cases, and $RP_{D2|D1} < 1.2$ for MSM in most cases (Fig. 4). To recollect, HIV prevalence was moderate for HETF, lowest for HETM, and high for MSM. Thus, there was no consistent pattern when comparing $RP_{D2|D1}$ and HIV disease burden (prevalence) alone. However, the pattern in $RP_{D2|D1}$ could be explained by the network structure as measured by average degree. In Scenario 1, for HETF, $d_{HIV+} > d_{overall}$, and $RP_{D2|D1} > 1.2$ if $d_{D2+} > d_{HIV+}$, and $RP_{D2|D1} \to 1$ as $d_{D2+} \to d_{overall}$ (Fig. 4c). For HETM, $d_{HIV+} < d_{overall}$ and $RP_{D2|D1} < 1$ in most cases. For MSM, $d_{HIV+} \gtrsim d_{overall}$ and $RP_{D2|D1} < 1.2$. This suggests that, when the average degree of both diseases is greater than the average degree in the overall population (as was the case for HETF in certain scenarios), $RP_{D2|D1}$ would be greater than 1, and if average degree of HIV is close to or less than the overall average degree (as was the case for HETM and MSM), then $RP_{D2|D1}$ would be closer to 1 or below 1.

The interpretation of the above results is that, when both diseases have a sufficiently low prevalence, they are both concentrated in higher-risk networks ($d_{D2+} > d_{overall}; d_{HIV+} > d_{overall}$) and thus, persons with HIV would have higher risk of Disease 2 co-infection. These conclusions are intuitive, and characteristic of scale-free networks, where the disease first spreads to high-risk networks before spreading to the rest of the network.

This correlation between $RP_{D2|D1}$ and patterns of average degree were consistent across the four scenarios, as discussed below, supporting the above conclusion. HETF and HETM in Scenario 2 *(low HIV prevalence low care)* had small decreases in HIV prevalence and saw minimal changes in $RP_{D2|D1}$ and average degrees (Fig. 4a). For MSM in Scenario 2, the lower HIV prevalence led to a concentration of disease burden in higher risk networks ($d_{HIV} > d_{overall}$)(Fig. 4c), and thus, the values of $RP_{D2|D1}$ tended to be higher (more reds) than in Scenario 1 (Fig. 4a). Compared to Scenario 2, though Scenario 3 *(low HIV prevalence high care)* created only minutely lower HIV prevalence, it had significantly lower HIV incidence because the higher

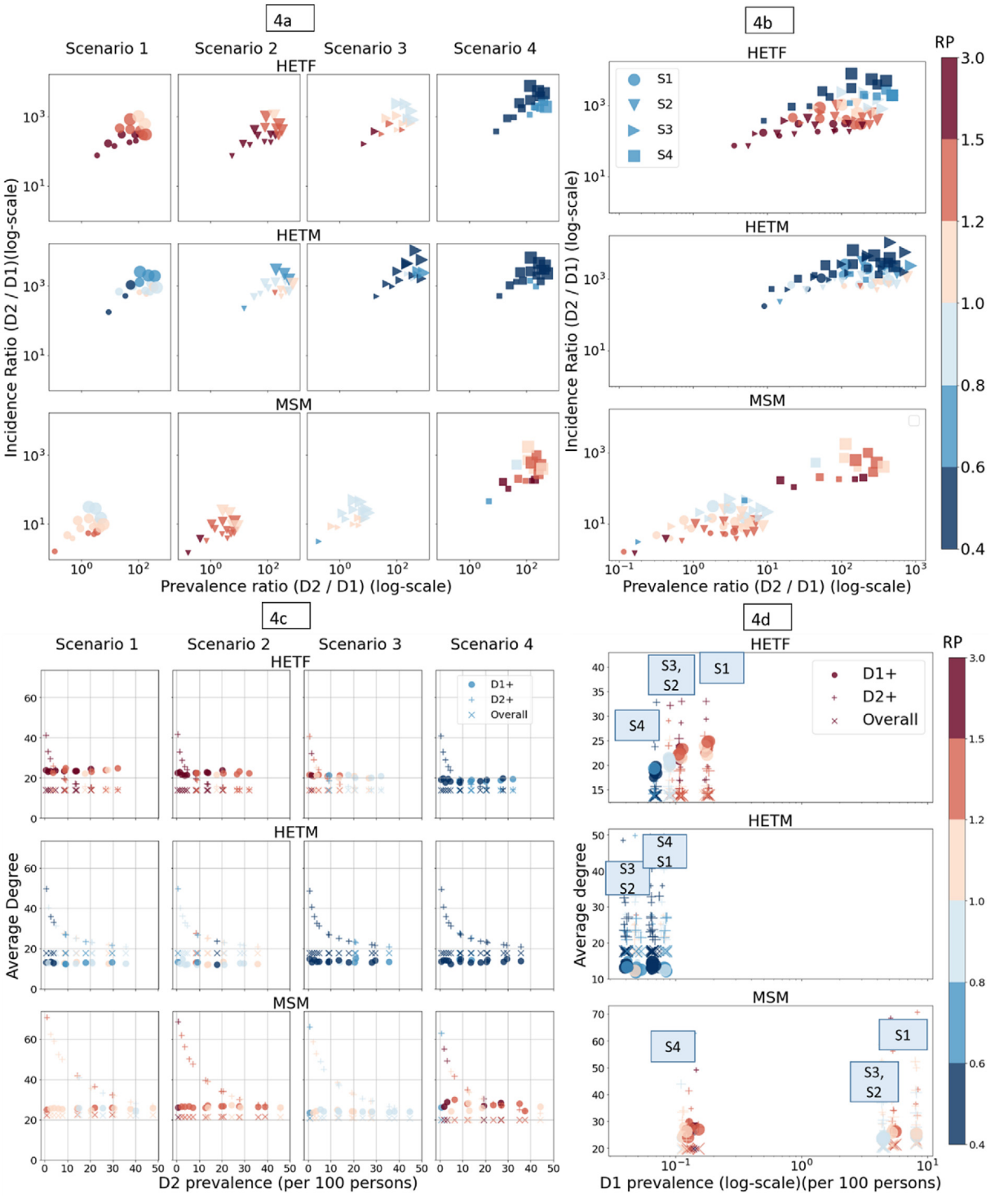

Fig. 4. a) Relative prevalence ($RP_{D2|D1}$) (color gradient) presented as a function of D2/D1 incidence ratio (y-axis) and prevalence ratio (x-axis) for Scenarios 1 to 4 in each column. b) Same as a) but all scenarios combined into one column. c) Corresponding average degrees (y-axis) among persons with at least D1 (D1+), at least D2 (D2+), and overall, plotted against D2 prevalence (x-axis) for Scenarios 1 to 4. d) The same average degrees (y-axis) but plotted against D1 prevalence; *$RP_{D2|D1}$ is the prevalence of D2 among persons with D1 compared to persons without D1;D1 is HIV; D2 is hypothetical Disease 2; HETF-heterosexual female; HETM-heterosexual male; MSM-men who have sex with men (men only and men and women). Note: For each HIV scenario (S1 to S4), there are 16 data points corresponding to each of the sixteen Disease 2 scenarios (larger the marker size higher the value of D2 transmission rate); Results are from last year of 12-year-long simulation (for S1 it corresponds to calendar year 2017).*

HIV-care led to fewer transmissions (Fig. 3b), leading in-turn to lower $RP_{D2|D1}$ for HETF and MSM. These changes in $RP_{D2|D1}$ could again be explained through corresponding changes in average degree. As average degree in HIV decreased and got closer to or equal to overall average degree ($d_{HIV} \sim d_{overall}$), $RP_{D2|D1}$ decreased to 1 or below. This also suggests that the reduction in transmissions from the higher HIV-care in Scenario 3 helped dissipate the impact of high HIV-prevalence burden in the high-risk networks.

In Scenario 4, HETM saw no change compared to Scenarios 1 to 3, it had a very low HIV prevalence and had $d_{HIV} < d_{overall}$. On the other hand, the $RP_{D2|D1}$ in HETF and MSM in Scenario 4 were opposite to that in Scenario 1, although both HETF and MSM saw a reduction in HIV prevalence in Scenario 4. For MSM, the average degree among HIV tended to be higher than overall ($d_{HIV} > d_{overall}$), suggesting that, because of the significantly lower HIV epidemic than in Scenario 1, it was now mostly concentrated in high-risk networks, and thus, $RP_{D2|D1} > 1$ when Disease 2 was also low and concentrated in high-risk network ($d_{D2} > d_{overall}$) (Fig. 4c). For HETF, though Scenario 4 initiated with the same HIV prevalence as Scenario 1, because of the mixing with MSM, it had a large reduction in HIV incidence and prevalence (Fig. 3b). The corresponding average degree among HIV was now closer to overall ($d_{HIV} \sim d_{overall}$), and thus the corresponding $RP_{D2|D1} < 1$ (Fig. 4c). These consistent patterns between relative prevalence and average degree, under varying values of HIV and Disease 2 burdens and care access, demonstrate the role of network features in burden of coinfection.

The behavior of $RP_{D1|D2}$ was similar to that of $RP_{D2|D1}$, i.e., if $RP_{D2|D1} > 1$ then $RP_{D1|D2} > 1$ (Fig. 5). These results again support that when both disease burdens are lower, the infection is more concentrated in higher risk networks.

4. Discussion

The purpose of this manuscript is to present a novel mixed agent-based compartmental (MAC) simulation framework for joint modeling of diseases with common modes of transmission but varying epidemiological features. The numerical analyses assessed the contribution of behavioral factors to joint-disease outcomes, and its sensitivity to disease burden, care metrics, and population heterogeneity and mixing. This work serves as a proof-of-concept for the feasibility of the proposed method and the sensitivity analyses highlights the potential significance of joint-disease modeling in a heterogeneous interacting population.

The key aspect of the MAC framework is its computational tractability while maintaining sufficient sample size even for lower prevalence diseases. The computational complexity of network modeling and compartmental modeling are in the $\mathcal{O}(N^2)$ and $\mathcal{O}(S)$, respectively, where N is the number of people simulated and S is the number of states. Thus, while compartmental modeling is computationally efficient, it lacks the granular individual–level features of network modeling, and while networks are favored for this feature, they are computationally complex and lose tractability as population size

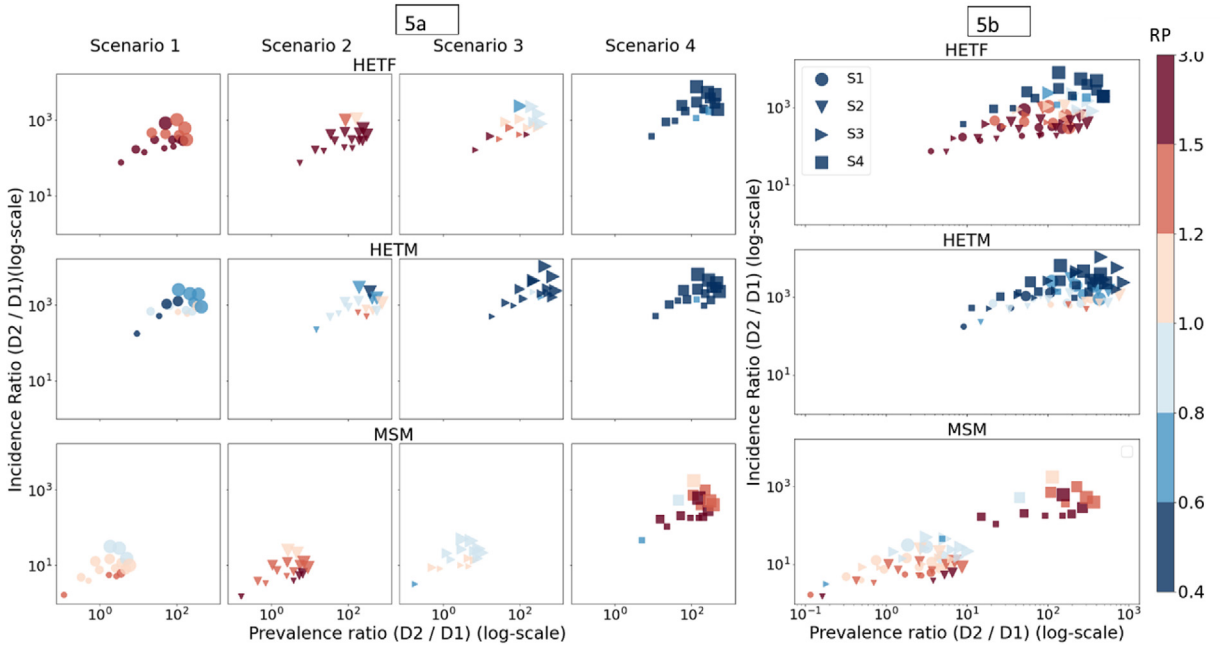

Fig. 5. a) Relative prevalence ($RP_{D1|D2}$)(color gradient) as a function of D2/D1 incidence ratio (y-axis) and prevalence ratio (x-axis) for Scenarios 1 to 4 (S1 to S4) in each column. b) Same as a) but all scenarios combined into one column; *$RP_{D1|D2}$ is the prevalence of D1 among persons with D2 compared to persons without D2; D1 is HIV; D2 is hypothetical Disease 2. HETF-heterosexual female; HETM-heterosexual male; MSM-men who have sex with men (men only and men and women). Note: For each HIV scenario (S1 to S4), there are 16 data points corresponding to each of the sixteen Disease 2 scenarios (larger the marker size higher the value of D2 transmission rate); Results are from last year of 12-year-long simulation (for S1 it corresponds to calendar year 2017).*

increases. The MAC simulation technique provides an efficient balance, as can be seen by sample computation times in Table 2. The computational complexity of MAC is in the $\mathcal{O}(Q_t + S + \theta I_t \bar{d}_n^2)$, where Q_t is the number of nodes in the network at time t, with upper bound equal to the number of infected nodes in the network (I_t) times the average number of lifetime partnerships per person ($\bar{d}_n$), and θ is an overall rate of infection, and thus θI_t is the number of newly infected nodes at time t. Note that an epidemiologically correct expression for new infections is $\frac{\theta I_t S_t}{N}$, where S_t is the number of susceptible persons, however, as only low prevalence diseases are modeled in the network, $S_t \cong N$. Also note that, because they are slow spreading diseases, θI_t is very small relative to I_t. Thus, unlike agent-based modeling where the computational complexity increases with N, here the computational complexity increases with I_t. This is a useful feature because the selection criteria for population size can be based on the desired sample size of positive cases without having to worry about its computational feasibility. For example, we can select the number of infected nodes in the network to be sufficiently large, say 12,000 (I_t). Then, simulating a disease with prevalence of 0.4% will generate a simulated population size of about 3 million persons (N), whereas, simulating a disease with prevalence of 0.2% will generate a simulated population size of about 6 million persons (N) but it will not increase the computational complexity. To achieve the same computational complexity when modeling two low prevalence diseases in the network, we can specify the total number of agents having one or both of the diseases. The resulting sample size would then depend on the prevalence of each and the overlap between the two diseases. For example, suppose the prevalence is 0.4% and 0.2% for two low prevalence diseases D1 and D2, respectively, and there is no overlap, i.e., each agent has one and only one of the two diseases. Generating 12,000 infected nodes will generate ~8000 persons with D1 and ~4000 persons with D2, and a total population of ~2 million. If these samples are not sufficient, then more nodes can be generated, with a concomitant non-linear increase in computation time that is closer to linear than quadratic. Note that in our numerical analyses we did not remove infected agents who were dead or remove partnerships that happened in the past. Doing so will not impact epidemic projections but can reduce computational time. The simulation technique here could also be useful to further improve efficiency of large-scale simulators that focus on software efficiencies and are capable of simulating millions as nodes in the network with the use of high performance computing (Bhatele et al., 2017; Grefenstette et al., 2013).

In the numerical analyses, the values of relative prevalence were greater than 1 in several scenarios, highlighting the influence of behavioral factors on joint disease outcomes. These values are lower than those reported from observational studies, e.g., a 4–8 fold increase in burden of cervical cancer caused by HPV infection was observed among women with HIV compared with women without HIV (Stelzle et al., 2021), and a 3 times higher HIV incidence risk was observed among MSM with rectal gonorrhea or chlamydia infection compared with MSM without these STIs (Pathela et al., 2013). The differences are expected because the data from the literature are estimates from cohort studies or case control studies and thus include risk of coinfection attributable to both biological factors and behavioral factors (Stelzle et al., 2021), whereas in the model we forced the biological risk to be zero so that relative prevalence is attributable to behavioral factors alone.

Consequently, through joint modeling of diseases, the differences between model estimates and observational studies can be used for determining risk attributed to biological factors alone and behavioral factors alone. These estimations can help inform both the type of interventions and optimal allocation of resources. While disease risk originating from behavioral factors would require behavioral and structural interventions because social determinants are key drivers of high-risk behaviors, disease risk originating from biological predisposition of pre-existing infections would additionally require disease management and care support programs. Using a model along with observational data to control for behavioral factors would help more realistically estimate the biological risk of acquisition and transmission of infections, and thus inform care management interventions. Modeling work in this area is limited (Chesson et al., 2016; Jones et al., 2019) and focused on modeling subgroups in isolation, such as MSM only. Our numerical analyses highlights the sensitivity of results in a subgroup to variations in disease burden in persons outside the subgroup due to population mixing, as in the comparison between Scenarios 4 and 2 for HETF.

While estimates of biological risk of co-infection can directly inform care management programs, and the estimates of risk attributable to behavioral factors are necessary for determining those biological risk estimates, the value of risk attributable to behavioral factors is not a sufficient measure for informing the need for behavioral and structural interventions. Indeed, values of relative prevalence closer to 1 or below could be generated because of higher HIV prevalence (MSM compared to HETF in Scenario 1), low HIV prevalence (HETM in all scenarios), mitigation of HIV risk through increased care access (Scenario 3 compared to Scenario 2 for HETF and MSM), or risk mitigation in the higher risk population when two groups mix (HETF in Scenario 4 compared to Scenario 2). Although the relative prevalence values were closer to 1 or below in all these

Table 2
Computational time of the mixed-agent based compartmental model for the two-disease example.

Number of nodes in the network			Number of persons in the compartmental model	Total simulation population size	[a]Computation time per run (minutes) Average (range)
Infected	Susceptible partners	Total			
4100	17,947	22,047	1,025,050	1,047,097	12(10-16)
8216	35,740	43,956	2,053,900	2,097,856	31(24-41)
12,020	50,612	62,632	3,005,000	3,067,632	56(46-71)

[a] Using single thread on Intel(R) Core(TM) i9-10900X CPU @ 3.70 GHz 3.70 GHz 64-bit operating system, x64-based processor. Average and range of 10 runs.

scenarios, structural interventions would be key interventions mainly in scenarios with high-prevalence and low care. Further, relative prevalence of greater than 1 can originate from factors within the population (comparing across Scenarios 1 to 4 for MSM) or from mixing with populations with high-risk of infection (HETF between Scenarios 2 and 4), each requiring different intervention strategies. Thus, although the values of relative prevalence would be necessary for inferring biological risk of infection, they alone are insufficient for informing interventions.

The above results from the numerical analyses justify the need for joint disease modeling for more accurate representation of the behavioral and biological dynamics of disease interactions. Further, social determinants, such as poverty, unemployment, homelessness, and stigma and discrimination, are known correlates of sexual and care behaviors that increase disease risk, such as higher number of partners, higher condomless sex, and lower treatment uptake among persons experiencing homelessness compared to persons with stable housing (Craddock et al., 2020; Edidin et al., 2012; Henwood et al., 2020; Maria et al., 2020). Therefore, structural interventions, such as healthcare coverage, subsidized housing and food programs, and access to mental healthcare, are key part of behavioral interventions to reduce risk of STI acquisition (Adimora & Auerbach, 2010; Blankenship et al., 2006; Frieden, 2010; Friedman et al., 1974; Sipe et al., 2017). While the costs of these structural interventions can be extrapolated from small cohort studies, the impact of structural interventions on disease burden is infeasible to estimate through controlled trials, because of the intricate disease interactions attributed to behavioral factors and its sensitivity to population and epidemic features (as observed through numerical analyses conducted here). A model would be a fundamental tool for estimation of the impact and thus cost-effectiveness, which are key measures used for allocation of public health resources. The new MAC simulation framework is computationally ideal for the above application, as it can be expanded to simulate sexual and care behavioral factors as a function of social conditions, and thus, subsequently serve as a decision-analytic tool for evaluation of structural interventions.

Joint modeling of STIs in the literature is limited, and most focus on sub population groups (Chesson et al., 2016; Jones et al., 2019). While sub-population modeling could help compare impact of alternate interventions on the sub-population, a national model that additionally simulates mixing between sub-populations and thus cross-over effects of interventions, would help identify optimal combination of interventions for overall reduction of diseases and disparities. Such a decision-analytic model would be suitable for informing public health guidelines, such as through the HealthyPeople2030 plan (, 2030Health Policy). Such a joint-disease joint-population model would also be suitable during emergence of new infection outbreaks, such as the recent 2022 Mpox outbreak. It could help shed light on populations at greatest risk and those that would benefit from medical countermeasures, to help inform interventions for containment of transmissions.

Our work is subject to limitations. The above analyses were conducted using hypothetical epidemiological and care assumptions, and thus, our work is limited to evaluating sensitivity of joint disease dynamics to key behavioral factors and epidemiological factors. Thus, the results should not be used to infer actual burden of coinfection. We assumed biological risk of coinfection to be zero to evaluate the sensitivity of behavioral factors alone. However, computational changes needed for modeling the biological risk are minimal, through use of a factor multiplied to the rates of transmission or progression to represent the increased risk, and calibrating the factor specific to a disease by matching simulated cases of coinfection with surveillance data. The scope of this work was limited to presenting a new simulation framework for joint modeling of diseases, and we did not model all behavioral changes driven from epidemic awareness. While some of these behavioral changes such as partnership selection for serosorting behaviors could be added to the current model structure through some modifications, changes in network structure, such as generational changes in the number of partners that would change the overall network statistics from the ones used in model calibration, would require recalibration. This would be a general challenge for any disease model and is outside the scope of this study. However, changes in network structure for evaluating impact of interventions could be carried out with the current model, by evaluating potential changes to network structure specific to interventions.

5. Conclusions

The study contributes a new simulation technique that is uniquely suitable for jointly modeling infectious diseases in a heterogeneous population that have common modes of transmission but varying epidemiological features, that a single simulation technique would be insufficient or computationally challenging. The numerical analysis serves as proof-of-concept for its application to STIs. The numerical analysis also demonstrates the influence of behavioral factors on joint disease outcomes, and its sensitivity to disease burden, care access, and population heterogeneity and mixing, which justify the need for joint modeling of related infectious diseases. Social and economic conditions are among key drivers of behaviors that increase STI risk. The new simulation framework is especially suitable for simulating behavioral factors as a function of social determinants, and it can be expanded in future work to subsequently evaluate optimal combinations of common structural interventions and disease-specific interventions for overall reduction of STI burden. The new simulation technique would also be suitable for the joint modeling of other infectious diseases that have common modes of transmissions. This would be especially suitable for early detection and intervention of new or emergent disease outbreaks, when prevalence is still low, but spread within networks of people with other ongoing diseases. Examples in recent years include Mpox for sexually transmitted infections, or COVID-19, SARS, MERS for respiratory infections.

Funding

Work was supported by the National Science Foundation, United States, under NSF 1915481 and the National Institute of Allergy and Infectious Diseases of the National Institutes of Health, United States, under Award Number R01AI127236. The funding agreement ensured the authors' independence in designing the study, interpreting the data, writing, and publishing the report.

Authors' contributions

CG was involved in conception of study, model development, analyses and interpretation of findings, and manuscript preparation. HB was involved in analyses and interpretation of findings, and manuscript preparation. PJH was involved in analyses and interpretation of findings, and manuscript preparation. All authors read and approved the final manuscript. HB and PJH equally contributed to the work and are listed in alphabetical order.

Declaration of competing interest

CG is also a Guest Researcher at the Division of HIV Prevention, Centers for Disease Control and Prevention. The findings and conclusions of this report are those of the authors and do not necessarily represent the official position of the Centers for Disease Control and Prevention. CG, HB, and PJH declare no other conflict of interest.

Acknowledgements

We like to acknowledge Drs. Melanie Taylor, Alexander Viguerie, Paul Farnham, Harrell Chesson, Emily Pollock, Cynthia Lyles, John Beltrami, and Anne-Marie France from the Centers for Disease Control and Prevention for their inputs on the manuscript.

Appendix A. Supplementary data

Supplementary data to this article can be found online at https://doi.org/10.1016/j.idm.2022.12.003.

List of Abbreviations

STIs	sexually transmitted infections
HIV	human immunodeficiency virus
HPV	human papillomavirus
HCV	hepatitis C
HBV	hepatitis B
NG	Gonorrhea
CT	Chlamydia
PWH	people with HIV
ART	antiretroviral therapy treatment
PrEP	pre-exposure prophylaxis
NHSS	U.S. National HIV Surveillance Systems
SDH	social determinants of health
MAC	mixed agent-based compartmental
ABENM	agent-based evolving network modeling
ABNM	agent-based network modeling
PATH 4.0	Progression and Transmission of HIV, version 4.0
ECNA	Evolving Contact Network Algorithm
RP	relative prevalence
HETF	heterosexual females
HETM	heterosexual males
MSM	men who have sex with men (men who have sex with men only and men who have sex with men and women)

References

Adimora, A. A., & Auerbach, J. D. (2010). Structural interventions for HIV prevention in the United States. *Journal of Acquired Immune Deficiency Syndromes, 55*, S132–S135.

Age and sex composition in the United States, United States census bureau. https://www.census.gov/data/tables/2017/demo/age-and-sex/2017-age-sex-composition.html [Last accessed August 2022].

Arias, E. (2004). United States life tables. *National Vital Statistics Reports, 56*(9), 1–40, 2007.

Bershteyn, A., Gerardin, J., Bridenbecker, D., Lorton, C. W., Bloedow, J., Baker, R. S., et al. (2018). Implementation and applications of EMOD, an individual-based multi-disease modeling platform. *Pathog Dis, 76*(5), fty059. Jul 1.

Bhatele, A., Yeom, J. S., Jain, N., Kuhlman, C. J., Livnat, Y., Bisset, K. R., et al. (2017). Massively parallel simulations of spread of infectious diseases over realistic social networks. In *2017 17th IEEE/ACM international symposium on cluster, cloud and grid computing (CCGRID) [internet]*. Madrid, Spain: IEEE [cited 2022 Dec 10]. pp. 689–94. Available from: http://ieeexplore.ieee.org/document/7973759/.

Bingham, A., Shrestha, R. K., Khurana, N., Jacobson, E. U., & Farnham, P. G. (2021). Estimated lifetime HIV-related medical costs in the United States. *Sexually Transmitted Diseases, 48*(4), 299–304. Apr 1.

Blankenship, K. M., Bray, S. J., & Merson, M. H. (2000). Structural interventions in public health. *AIDS, 14*(Suppl 1), S11–S21.

Blankenship, K. M., Friedman, S. R., Dworkin, S., & Mantell, J. E. (2006). Structural interventions: Concepts, challenges and opportunities for research. *J Urban Health Bull N Y Acad Med, 83*(1), 59–72.

Board, A. R., Oster, A. M., Song, R., Gant, Z., Linley, L., Watson, M., et al. (1999). Geographic distribution of HIV transmission networks in the United States. *Journal of Acquired Immune Deficiency Syndromes, 85*(3), e32–e40, 2020 Nov 1.

Broz, D., Wejnert, C., Pham, H. T., DiNenno, E., Heffelfinger, J. D., Cribbin, M., et al. (2009). HIV infection and risk, prevention, and testing behaviors among injecting drug users – National HIV Behavioral Surveillance System, 20 U.S. cities. *Morb Mortal Wkly ReportSurveillance Summ Wash DC 2002, 63*(6), 1–51, 2014.

Buchacz, K., Armon, C., Palella, F. J., Baker, R. K., Tedaldi, E., Durham, M. D., et al. (2012). CD4 cell counts at HIV diagnosis among HIV Outpatient Study participants, 2000-2009. *AIDS Res Treat, 2012*, Article 869841.

hiv-surveillance-special-report-number-25.pdf [Internet]. [cited 2021 Nov 20]. Available from: cdc https://www.cdc.gov/hiv/pdf/library/reports/surveillance/cdc-hiv-surveillance-special-report-number-25.pdf.

Centers for Disease Control and Prevention. (2015). Estimated HIV incidence and prevalence in the United States. In *2019. HIV surveillance supplemental report 2021, 26*. No. 1 http://www.cdc.gov/hiv/library/reports/hiv-surveillance.html. Published May 2021. Accessed [11/20/201].

Centers for Disease Control and Prevention. HIV surveillance reports. https://www.cdc.gov/hiv/library/reports/hiv-surveillance.html [Last Accessed August 2022].

Centers for Disease Control and Prevention. Atlas plus. https://www.cdc.gov/nchhstp/atlas/about-atlas.html. Last Accessed August 2022].

Centers for Disease Control and Prevention. (2013). Monitoring selected national HIV prevention and care objectives by using HIV surveillance data—United States and 6 dependent areas—2011. *HIV Surveillance Supplemental Report, 18*(No. 5). http://www.cdc.gov/hiv/library/reports/surveillance/. Published October 2013. Accessed August 2022. (Journal Article).

Centers for Disease Control and Prevention. (2017). Monitoring selected national HIV prevention and care objectives by using HIV surveillance data—United States and 6 dependent areas, 2015. *HIV Surveillance Supplemental Report, 22*(No. 2). Published July 2017. Accessed [August 2022]. (Journal Article) http://www.cdc.gov/hiv/library/reports/hivsurveillance.html.

Centers for Disease Control and Prevention. (2018). Estimated HIV incidence and prevalence in the United States, 2010–2015. *HIV Surveill Suppl Rep, 23*(No. 1). Journal Article) http://www.cdc.gov/hiv/library/reports/hiv-2018.

Centers for Disease Control and Prevention. (2022). Monitoring selected national HIV prevention and care objectives by using HIV surveillance data—United States and 6 dependent areas, 2020. *HIV Surveillance Supplemental Report, 27*(No. 3). http://www.cdc.gov/hiv/library/reports/hiv-surveillance.html. Published May 2022. Accessed [August 2022].

Centers for Disease C Prevention. (2010). Vital signs: HIV testing and diagnosis among adults–United States, 2001-2009. *MMWR Morb Mortal Wkly Rep, 59*(47), 1550–1555.

Centers for Disease C Prevention. (2011). HIV surveillance–United States, 1981-2008. *MMWR Morb Mortal Rep, 60*(21), 689–693.

Chandra, A., Mosher, W. D., Copen, C., & Sionean, C. (2011). Sexual behavior, sexual attraction, and sexual identity in the United States: Data from the 2006-2008 national survey of family Growth. *Natl Health Stat Rep, 2011/05/13*(36), 1–36.

Chan, P. A., Robinette, A., Montgomery, M., Almonte, A., Cu-Uvin, S., Lonks, J. R., et al. (2016). Extragenital infections caused by Chlamydia trachomatis and Neisseria gonorrhoeae: A review of the literature. *Infectious Diseases in Obstetrics and Gynecology, 2016*, Article 5758387.

Chesson, H. W., Kidd, S., Bernstein, K. T., Fanfair, R. N., & Gift, T. L. (2016). The cost-effectiveness of syphilis screening among men who have sex with men: An exploratory modeling analysis. *Sexually Transmitted Diseases, 43*(7), 429–432. Jul.

Chesson, H. W., Spicknall, I. H., Bingham, A., Brisson, M., Eppink, S. T., Farnham, P. G., et al. (2021). The estimated direct lifetime medical costs of sexually transmitted infections acquired in the United States in 2018. *Sexually Transmitted Diseases, 48*(4), 215–221. Apr.

Craddock, J., Barman-Adhikari, A., Combs, K. M., Fulginiti, A., & Rice, E. (2020). Individual and social network correlates of sexual health communication among youth experiencing homelessness. *AIDS and Behavior, 24*(1), 222–232. Jan.

Damery, S., Flanagan, S., & Combes, G. (2015). The effectiveness of interventions to achieve co-ordinated multidisciplinary care and reduce hospital use for people with chronic diseases: Study protocol for a systematic review of reviews. *Systematic Reviews, 4*(64).

Eden, M., Castonguay, R., Munkhbat, B., Balasubramanian, H., & Gopalappa, C. (2021). Agent-based evolving network modeling: A new simulation method for modeling low prevalence infectious diseases. *Health Care Management Science, 24*(3), 623–639. Sep.

Edidin, J. P., Ganim, Z., Hunter, S. J., & Karnik, N. S. (2012). The mental and physical health of homeless youth: A literature review. *Child Psychiatry and Human Development, 43*(3), 354–375. Jun.

Ferenczy, A., Coutlee, F., Franco, E., & Hankins, C. (2003). Human papillomavirus and HIV coinfection and the risk of neoplasias of the lower genital tract: A review of recent developments. *CMAJ (Canadian Medical Association Journal) Journal de l'Association Medicale Canadienne, 169*(5), 431–434.

Finlayson, T. J., Le, B., Smith, A., Bowles, K., Cribbin, M., Miles, I., et al. (2011). HIV risk, prevention, and testing behaviors among men who have sex with men–National HIV Behavioral Surveillance System, 21 U.S. cities, United States, 2008. *MMWR Surveill Summ Morb Mortal Wkly Rep Surveill Summ CDC, 60*(14), 1–34.

Fleming, D. T., & Wasserheit, J. N. (1999). From epidemiological synergy to public health policy and practice: The contribution of other sexually transmitted diseases to sexual transmission of HIV infection. *Sexually Transmitted Infections, 75*(1), 3–17. Feb 1.

Frieden, T. R. (2010). A framework for public health action: The health impact pyramid. *American Journal of Public Health, 100*(4), 590–595.

Friedman, E. E., Dean, H. D., & Duffus, W. A. (1974). Incorporation of social determinants of health in the peer-reviewed literature: A systematic review of articles authored by the national center for HIV/aids, viral hepatitis, std, and tb prevention. *Public Health Report Wash DC, 133*(4), 392–412, 2018 Aug.

Friedman, M. R., Wei, C., Klem, M. L., Silvestre, A. J., Markovic, N., & Stall, R. (2014). HIV infection and sexual risk among men who have sex with men and women (MSMW): A systematic review and meta-analysis. *PLoS One, 9*(1), Article e87139.

Glick, S. N., Morris, M., Foxman, B., Aral, S. O., Manhart, L. E., Holmes, K. K., et al. (2012). A comparison of sexual behavior patterns among men who have sex with men and heterosexual men and women. *Journal of Acquired Immune Deficiency Syndromes, 60*(1), 83–90. May 1.

Grefenstette, J. J., Brown, S. T., Rosenfeld, R., DePasse, J., Stone, N. T., Cooley, P. C., et al. (2013). FRED (a framework for reconstructing epidemic dynamics): An open-source software system for modeling infectious diseases and control strategies using census-based populations. *BMC Public Health, 13*. Journal Article):940–940.

Health Policy. Healthy people 2030, Department of Health and Human Services. https://health.gov/healthypeople/objectives-and-data/browse-objectives/health-policy [last accessed August 2022].

Heiligenberg, M., Rijnders, B., Schim van der Loeff, M. F., de Vries, H. J. C., van der Meijden, W. I., Geerlings, S. E., et al. (2012). High prevalence of sexually transmitted infections in HIV-infected men during routine outpatient visits in The Netherlands. *Sexually Transmitted Diseases, 39*(1), 8–15. Jan.

Henwood, B. F., Rhoades, H., Redline, B., Dzubur, E., & Wenzel, S. (2020). Risk behaviour and access to HIV/AIDS prevention services among formerly homeless young adults living in housing programmes. *AIDS Care, 32*(11), 1457–1461. Nov.

Huang, Y. L., Frazier, E. L., Sansom, S. L., Farnham, P. G., Shrestha, R. K., Hutchinson, A. B., et al. (2015). Nearly half of US adults living with HIV received federal disability benefits in 2009. *Health Aff Proj Hope, 34*(10), 1657–1665.

Jeon, Y. H., Black, A., Govett, J., Yen, L., & McRae, I. (2012). Private health insurance and quality of life: Perspectives of older Australians with multiple chronic conditions. *Australian Journal of Primary Health, 18*(3), 212–219.
Jones, J., Weiss, K., Mermin, J., Dietz, P., Rosenberg, E. S., Gift, T. L., et al. (2019). Proportion of incident human immunodeficiency virus cases among men who have sex with men attributable to gonorrhea and Chlamydia: A modeling analysis. *Sexually Transmitted Diseases, 46*(6), 357–363. Jun.
Kreisel, K. M., Spicknall, I. H., Gargano, J. W., Lewis, F. M. T., Lewis, R. M., Markowitz, L. E., et al. (2018). Sexually transmitted infections among US women and men: Prevalence and incidence estimates. *Sexually Transmitted Diseases, 48*(4), 208–214, 2021 Apr.
Lauer, J. A., Rohrich, K., Wirth, H., Charette, C., Gribble, S., & Murray, C. J. (2003). PopMod: A longitudinal population model with two interacting disease states. *Cost Eff Resour Alloc CE, 1*(1), 6.
Liljeros, F., Edling, C. R., Amaral, L. A. N., Stanley, H. E., & Åberg, Y. (2001). The web of human sexual contacts. *Nature, 411*(6840), 907–908.
Lin, K. Y., Sun, H. Y., Lee, T. F., Chuang, Y. C., Wu, U. I., Liu, W. C., et al. (2021). High prevalence of sexually transmitted coinfections among at-risk people living with HIV. *Journal of the Formosan Medical Association Taiwan Yi Zhi, 120*(10), 1876–1883. Oct.
Liu, H. F., Liu, M., & Xu, Y. L. (2016). Analysis of high-risk HPV infection and cervical cytologic screening in HIV positive women. *Zhonghua Fu Chan Ke Za Zhi, 51*(10), 734–738.
Liu, G., Sharma, M., Tan, N., & Barnabas, R. V. (2018). HIV-positive women have higher risk of human papilloma virus infection, precancerous lesions, and cervical cancer. *AIDS Lond Engl, 32*(6), 795–808. Mar 27.
Maria, D. S., Daundasekara, S. S., Hernandez, D. C., Zhang, W., & Narendorf, S. C. (2020). Sexual risk classes among youth experiencing homelessness: Relation to childhood adversities, current mental symptoms, substance use, and HIV testing. *PLoS One, 15*(1), Article e0227331. Jan 3.
McPhail, S. M. (2016). Multimorbidity in chronic disease: Impact on health care resources and costs. *Risk Management and Healthcare Policy, 9*, 143–156. Journal Article).
Ong, J. J., Baggaley, R. C., Wi, T. E., Tucker, J. D., Fu, H., Smith, M. K., et al. (2019). Global epidemiologic characteristics of sexually transmitted infections among individuals using preexposure prophylaxis for the prevention of HIV infection: A systematic review and meta-analysis. *JAMA Network Open, 2*(12), Article e1917134. Dec 11.
Orroth, K. K., White, R. G., Korenromp, E. L., Bakker, R., Changalucha, J., Habbema, J. D. F., et al. (2006). Empirical observations underestimate the proportion of human immunodeficiency virus infections attributable to sexually transmitted diseases in the mwanza and rakai sexually transmitted disease treatment trials: Simulation results. *Sexually Transmitted Diseases, 33*(9), 536–544.
Pathela, P., Braunstein, S. L., Blank, S., & Schillinger, J. A. (2013). HIV incidence among men with and those without sexually transmitted rectal infections: Estimates from matching against an HIV case registry. *Clin Infect Dis Off Publ Infect Dis Soc Am, 57*(8), 1203–1209. Oct.
Paul, J. A., MacDonald, L., & Hariharan, G. (2014). Modeling risk factors and disease conditions to study associated lifetime medical costs. *Service Science, 6*(1), 47.
Prejean, J., Song, R., Hernandez, A., Ziebell, R., Green, T., Walker, F., et al. (2011). Estimated HIV incidence in the United States, 2006-2009. *PLoS One, 6*(8), Article e17502.
Purcell, D. W., Johnson, C. H., Lansky, A., Prejean, J., Stein, R., Denning, P., et al. (2012). Estimating the population size of men who have sex with men in the United States to obtain HIV and syphilis rates. *The Open AIDS Journal, 6*, 98–107. Journal Article).
Reece, M., Herbenick, D., Schick, V., Sanders, S. A., Dodge, B., & Fortenberry, J. D. (2010). Background and considerations on the national survey of sexual health and behavior (NSSHB) from the investigators. *The Journal of Sexual Medicine, 7*(Suppl 5), 243–245.
Singh, S., France, A. M., Chen, Y. H., Farnham, P. G., Oster, A. M., & Gopalappa, C. (2021). Progression and transmission of HIV (PATH 4.0)-A new agent-based evolving network simulation for modeling HIV transmission clusters. *Mathematical Biosciences and Engineering, 18*(3), 2150–2181. Mar 3.
Sipe, T. A., Barham, T. L., Johnson, W. D., Joseph, H. A., Tungol-Ashmon, M. L., & O'Leary, A. (2017). Structural interventions in HIV prevention: A taxonomy and descriptive systematic review. *AIDS and Behavior, 21*(12), 3366–3430.
Smieszek, T., Fiebig, L., & Scholz, R. W. (2009). Models of epidemics: When contact repetition and clustering should be included. *Theoretical Biology and Medical Modelling, 6*. Journal Article):11–11.
Stelzle, D., Tanaka, L. F., Lee, K. K., Ibrahim Khalil, A., Baussano, I., Shah, A. S. V., et al. (2021). Estimates of the global burden of cervical cancer associated with HIV. *Lancet Global Health, 9*(2), e161–e169. Feb.
Tartaglia, E., Falasca, K., Vecchiet, J., Sabusco, G. P., Picciano, G., Di Marco, R., et al. (2017). Prevalence of HPV infection among HIV-positive and HIV-negative women in Central/Eastern Italy: Strategies of prevention. *Oncology Letters, 14*(6), 7629–7635. Dec.
Thio, C. L., Seaberg, E. C., Skolasky, R., Jr., Phair, J., Visscher, B., Munoz, A., et al. (2002). HIV-1, hepatitis B virus, and risk of liver-related mortality in the Multicenter Cohort Study (MACS). *Lancet Lond Engl, 360*(9349), 1921–1926.
Tsuboi, M., Evans, J., Davies, E. P., Rowley, J., Korenromp, E. L., Clayton, T., et al. (2021). Prevalence of syphilis among men who have sex with men: A global systematic review and meta-analysis from 2000-20. *Lancet Global Health, 9*(8), e1110–e1118. Aug.
Voetsch, A. C., Lansky, A., Drake, A. J., MacKellar, D., Bingham, T. A., Oster, A. M., et al. (2012). Comparison of demographic and behavioral characteristics of men who have sex with men by enrollment venue type in the National HIV Behavioral Surveillance System. *Sexually Transmitted Diseases, 39*(3), 229–235.
Journal Article Walker, N., Tam, Y., & Friberg, I. K. (2013). Overview of the lives saved tool (LiST). *BMC Public Health, 13*(Suppl 3). S1-S1. Epub 2013 Sep. 17.
Werner, R. N., Gaskins, M., Nast, A., & Dressler, C. (2018). Incidence of sexually transmitted infections in men who have sex with men and who are at substantial risk of HIV infection – a meta-analysis of data from trials and observational studies of HIV pre-exposure prophylaxis. Mugo PM. *PLoS One, 13*(12), Article e0208107. Dec 3.
World Health Organization. (2013). *OneHealth Tool: Supporting integrated strategic health planning, costing and health impact analysis*. World Health Organization. https://www.who.int/tools/onehealth (last accessed August 2022).